

# The All Sky Automated Survey<sup>1</sup>

by

G. Pojmański

Warsaw University Observatory Al Ujazdowskie 4, 00-478 Warsaw, Poland

## ABSTRACT

Technical description of the new project called All Sky Automated Survey and results of the tests of our prototype instrument are presented. The ultimate goal of this project is photometric monitoring of the large area of the sky with fully automated, low cost instruments. Possible applications of the project are indicated and future prospects discussed. At present over hundred square degrees is observed 5–10 times each night in *I* band, allowing us to monitor over 30 000 stars brighter than 12–13 mag. Full description, pictures and current status of the project can be found on the WWW: <http://sirius.astrouw.edu.pl/~gp/asas/asas.html>

**Key words:** *Surveys-Telescopes- Techniques:photometric*

## 1 Introduction

Availability of the large CCD detectors allowed astronomers to start the new age of massive survey projects. Most of them propose to search for some kind of specific objects or events. Among them are microlensing groups: OGLE (Udalski *et al.* 1992), MACHO (Alcock *et al.* 1993) and EROS (Aubourg *et al.* 1993), searches for the optical counterparts of gamma-ray bursts, supernovae searches (BAIT, Van Dyk *et al.* 1994) and projects interested in variable stars, near-Earth asteroids, comets, like All Sky Patrol Astrophysics (Braeuer and Vogt 1995). At least part of these activities are expected to be performed in the automated way. Some are already done by robotic telescopes (Hayes and Genet 1989, Schaefer *et al.* 1994, Henry and Eaton 1995).

---

<sup>1</sup>Based on observations obtained at the Las Campanas Observatory of the Carnegie Institution of Washington.

Many interesting scientific programs can be done even with surveys covering only the brightest of the observable objects (Paczynski 1997). The main topics include variable stars, comets, asteroids and near-Earth objects, supernovae or AGNs.

In this paper we present a description of the new observational project called All Sky Automated Survey which we have started at the beginning of 1996.

The ultimate goal of our project is to detect and investigate any kind of the photometric variability present on as much of the sky as possible. At the beginning we restrict ourselves only to the brightest few million stars on the sky, *i.e.*, our magnitude limit is about 13 mag. We will increase this limit in future, as our data acquisition and data processing capabilities grow. We want to achieve this aim at relatively low cost, using simple but powerful automatic modules linked together at the observing sites with good weather conditions.

## 2 Prototype Instrument

The prototype instrument was built in 1996 at the Warsaw University Observatory. It consists of five basic elements: equatorial mount, CCD camera, telephoto lens, electronic box and control computer.

### 2.1 Mount

Equatorial mount is a compact, lightweight (aluminum alloy) horseshoe design similar to those built by AutoScope (Genet and Hayes 1989). It consists of the base structure with right ascension drive, horseshoe with declination drive and camera platform.

The triangular base rests on the adjustment table. Polar vertex has a precise vertical screw used for adjustment of the inclination of polar axis. Spherical bearing supporting polar axle is mounted on the upper side of this vertex. The other two vertices have horizontal screws used for precise horizontal alignment. Two roller holders extend from these vertices. Each contains two bearings and steel roller on which horseshoe rests. One roller runs idle while the other, linked to the the RA stepper motor through intermediary sprocket gears drives the horseshoe *via* friction.

The horseshoe assembly has three arms of approximately 500 mm length, connected at one end to form a polar axle. Two declination axle supports are mounted on the front side of the horseshoe while on the back side declination sprocket gears and stepper motor are located.

Stepper motors are driven by the electronic box, containing power supplies, microprocessor controllers and translator drives. Both stepper motors are controlled over the same serial link.

RA drive transmission rate (including friction roller and horseshoe) is approximately 950:1 which leads to the RA resolution of 3.4 arcsec per step. It requires

about four steps per second to track the sky rotation. Sprocket gears and friction roller form a non-backlash drive with positioning repeatability much better than one arcsec.

Declination drive has much smaller gear rate – 28.8:1 – and therefore each motor step corresponds to 112.5 arcsec. Positioning accuracy in declination at different hour angles is reduced to a few tens of arcsec due to the lack of friction element and long elastic chain belts.

Maximum slewing rate is about 5 deg/sec in hour angle and 150 deg/sec in declination. Therefore the average pointing time during a regular observing run is about 10 seconds.

Instrument platform of 280 mm diameter, hanging on two declination half-shafts, has mounting holes for three CCD cameras. The prototype has only one CCD system mounted. The total weight of the instruments mounted on the platform should not exceed 15 kg and the outline of the back side of the instrument should stay within the half-sphere of 170 mm radius.

## 2.2 CCD Camera System

CCD camera is a commercial Meade Pictor 416 product with Kodak KAF 0400 chip. It has  $516 \times 768$  pixels of 9 micron size with full well capacity of 85000 electrons. The only available gain of the system is  $1.2 \text{ ADU}/e^-$  and therefore pixel counts are easily stored as 2 byte integers. Factory data claim 42% peak quantum efficiency. CCD head has a two-stage thermoelectric cooler capable to cool CCD down to 45 degrees below the case temperature.

Pictor 416 camera has its own electronic box controlling cooling, exposing and data acquisition. It is accessible from the interactive PC software *via* SCSI or RS-232 interfaces. Since we needed a direct control over the camera we have added our own driver for the fast (110 kbauds) serial link. This serial link is presently a bottle-neck of our system. Transfer time of the full image to the main computer is equal to 40-80 sec, while the Pictor electronics itself reads CCD chip in 4 seconds only.

Camera head has built-in two-leaf fast shutter which failed after a few thousand exposures.

We have equipped our camera with 135/1.8 Sigmatel lens which gives the scale of 14.2 arcsec/pixel and  $3 \times 2$  deg field of view. Telephoto lens proved to have very unpleasant, triangular point spread function but produces very little of field distortions. With such fast lens our CCD system is sky limited and exposure times are limited to a few minutes.

There is some space for a filter between the lens and camera head. Currently *I*-band filter (Schott RG-9, 3 mm) is used.

The mount, camera and electronic box are housed in the  $0.6 \text{ m} \times 0.6 \text{ m} \times 0.8 \text{ m}$  water-proof ply-wood box, which has to be manually closed in case of bad weather.

Polar axis of the mount can be adjusted for any latitude between 18 and 54 degrees (North or South). For other latitudes special supporting frame is needed.

### 2.3 Control Computer

The control computer is SparcStation 5 with 64 MB RAM, 9 GB disk space and DAT-2 tape drive.

The heart of the control software is a remotely accessible database server, which keeps all necessary information about the system and distributes it to the interested clients. There are three main database clients: camera driver communicating with the Pictor system over the fast serial link, motor driver communicating with the mount over the slow serial link and "observer" program managing observations. There is also image server sending images to the interested clients (usually in the interactive mode) and "analyst" client which manages data reduction process.

## 3 Observation Schedule

Automated observations begin at 5 p.m. when computer initiates "observer" program. This in turn performs system checkup and schedules start of observation for a few minutes before dusk. Camera cooling is then switched on and the system waits for the Sun to hide a few degrees below horizon. At this time camera is pointed into zenith and a set of sky flat field images is obtained. When the sky is too dark for flat field images, "observer" takes a few dark frames and waits until the end of twilight.

Then regular observations start. "Observer" loops over a list of selected fields checking each time visibility conditions. If the field is invisible or too low, is obscured by the surrounding obstacles (dome and house) or is too close to the Moon – it is skipped. If visibility conditions are satisfied camera is moved into desired position and the shutter is opened.

Exposure lasts for three minutes. Then camera electronics reads out new frame and transfers it to the computer. New image is immediately stored on the disk and database server gets informed about completing the observation. This information is forwarded to the "analyst" program, which starts frame reduction process. Afterwards "observer" checks the Sun position and if it is still well below horizon – goes to the next field on the list. Otherwise it starts shutdown procedure and starts data dump to the DAT-2 tape. Such a schedule results in about 20 calibration frames and 120 program frames each night, creating data stream of 120 MB per night.

Observing schedule is flexible. In principle it is possible to change or add "on fly" observed targets remotely, using Internet and database server. At present system requires human interaction only for emergency closing in the bad weather conditions and for changing the DAT tape once a month.

## 4 Data Reduction

At the beginning of the night the "analyst" program waits for the dark exposures to be completed. Then it calculates medianed dark frame and, using recent sky-flat frames, it computes new flat-field image. Dark and flat-field frames are given unique names and stored in a special directory. On some nights (*e.g.*, if observations start late) new dark or flat frames may not be created.

During regular observations "analyst" sleeps until new frame is saved to the disk. Then it performs (depending on the current settings) some of the following tasks: dark subtraction, flat-fielding, object detection, photometry, astrometry and catalog updating.

Dark subtraction and flat division are performed using the latest available dark and flat images (usually from the beginning of the night).

Object detection program looks at the image intensity enhancements and tries to classify them as stars, galaxies, cosmic rays and various trails. It is based on the DAOPHOT algorithm (Stetson 1987), *i.e.*, it convolves image with the lowered, truncated point spread function and then searches for the local maxima above pre-selected threshold. Object classification is done using "sharpness" and "roundness" attributes. Special treatment is required for the elongated trails.

Objects classified as stars and galaxies are then subject to photometry. After many experiments with various photometry schemes we decided to stay with aperture photometry during the prototype phase of our project. It is much faster and more reliable with our non-symmetric PSF (see Section 7.1).

Astrometry program uses Guide Star Catalog as a source of accurate stellar positions. Depending on the field crowding there are between 100 and 1000 GSC stars present on each frame. For astrometry solution, which in our case proved to require only rotation, translation and scaling, we use only a few hundred brightest stars. The rms distance between GSC stars and matching stars usually converges to 0.2 pixel (3 arcsec).

## 5 The Catalog

### 5.1 Structure

Results of the photometry obtained for stars and galaxies are put into the photometric catalog which is arranged as a relational database that consists of four types of files.

The first one (FLOG) is an observation log updated as soon as frame exposure is completed. Each record (about 100 bytes long) contains sequential frame number, time of observation, coordinates of the frame center, camera and site information, exposure details, reduction status, quality classification, photometry and astrometry transformation coefficients and link to the photometry file.

Main catalog file (CAT) forms a tree structured database in which records (32 bytes long) are sorted by declination and right ascension. Such construction is very flexible although not very fast. New objects are entered at the end of the file and only two internal links have to be updated to properly sort the database. To access selected object one needs to follow (read) about  $\log_2 N$  records from the database (where  $N$  is the number of objects in the database). At present we are able to search a few hundred objects per second. Each CAT record contains  $\alpha$  and  $\delta$  (2000) coordinates of the object, average magnitude and its dispersion, classification and pointer to the LINK file.

Link database (LINK) chains photometry entries for each catalog object. Each record (12 bytes long) contains pointer to the FLOG file (giving access to the frame details, *e.g.*, HJD of exposure and transformation coefficients), pointer to the PHOTO file (raw magnitudes) and pointer to the next LINK record for the same object.

Photometry file (PHOTO) is a continuous storage for the photometry results. Each record (10 bytes long) contains the following information for the detected objects: pointer to the main catalog (CAT) entry, coordinate offsets from that entry, raw magnitude and its error, classification details.

LOG and CAT file are relatively small and therefore only one instant of each exists. Photometry and link files grow very fast (a few MB per night) and therefore we are prepared to keep multiple PHOTO and LINK files distributed over the network.

## 5.2 Catalog Interface and Data Calibration

Extended C-language library forms an interface to the database which allows user to add, delete, search and retrieve data. Many different filters could be applied (*e.g.*, coordinate and magnitude limits, data scattering, number of observations) to retrieve only the most relevant information. Graphical user interface on the WWW page can be used to access some catalog data from the Internet (<http://www.astro.uw.edu.pl/~gp/asas/catalogue.html>).

The most important procedure in the library is "add\_ast" program that puts astrometry results into the catalog. Since we want our catalog magnitudes  $I_{\text{cat}}$  to be as close to the standard system as possible, we have to convert instrumental magnitudes  $i$  using standard transformation (without color terms):

$$I_{\text{cat}} = i + i_0 + k_I X \quad (1)$$

where  $i_0$  denotes instrumental offset and  $k_I$  extinction coefficient.

In practice it is enough to perform this calibration only once for each field. It requires frames obtained during dark, photometric nights, for which extinction coefficient  $k_I$  is stable and well known. This task has not yet been fully automated - requires user to select the best frames for calibration.

Adding photometry results for the already calibrated fields is performed in two steps.

First the catalog is searched for each object on the astrometry list. If coordinate match within specified radius (usually 15 arcsec) is found, the catalog data are retrieved and tested. If the object contains saturated pixels, is unusually elongated, marked as variable or too faint – it is rejected. Otherwise it is added to the matching list.

In the second step differences  $I_{\text{cat}} - i$  (catalog magnitude *minus* raw magnitude) are calculated for the matching stars, and the least squares method is used to find best  $i_0$  and  $k_I$  coefficients. Fit residua are then inspected and deviating values rejected. The whole procedure is repeated until satisfactory convergence is achieved.

Such general attitude is required only if substantial differential extinction effects are expected. If this is not the case than two other program options could be used. First option uses fixed extinction coefficient  $k_I$  (determined from the observation of the same field at different zenith distances) and solves transformation equation for  $i_0$ . The second option neglects differential extinction on the frame and solves transformation for the whole  $\Delta i = i_0 + k_I \bar{X}$  term, where  $\bar{X}$  is an average air mass for the frame.

Field of view of our prototype instrument is  $2 \times 3$  degrees and therefore differential extinction in  $I$ -band is always smaller than 0.01 mag. Having other sources of larger errors we decided to use last option for magnitude transformation. General method will be applied in the next phase of experiment, when 2k by 2k CCD detectors will be used.

Calibration has not to be done immediately after observation. In fact raw magnitudes are stored in the PHOT database and only the calibration coefficients are saved for each frame in the FLOG records.

## 6 System Integrity Tests

The prototype was assembled and tested at the Warsaw University Observatory in fall/winter 1996.

CCD tests proved that Pictor 416 system produced acceptable images with readout noise of 9 electrons and good linearity. Chip surface was clean and only a few dark spots were visible on the flat field images. Electronic interference pattern was visible on some dark frames, but its intensity was smaller than the read-out noise. Dark frames revealed also some distinct populations of hot pixels. At CCD temperature of  $-12^\circ\text{C}$ , 6% of all pixels have dark current less than  $25\text{ e}^-/\text{min}$ , and only 0.1% larger than  $40\text{ e}^-/\text{min}$ . There are also more than 50 pixels with dark current larger than  $1000\text{ e}^-/\text{min}$ . The shutter error was not important for exposure times longer than 0.5 sec.

At the beginning of the test the thermocooler was able to cool the CCD  $42^\circ\text{C}$

below the case temperature. However, at 80% cooling efficiency the camera head went  $10^{\circ}\text{C}$  above the ambient. Therefore small fan was added to keep the head case temperature within ambient  $+5$  deg limit. At the average night conditions ( $+15^{\circ}\text{C}$ ) the CCD detector was kept typically at  $-20^{\circ}\text{C}$ .

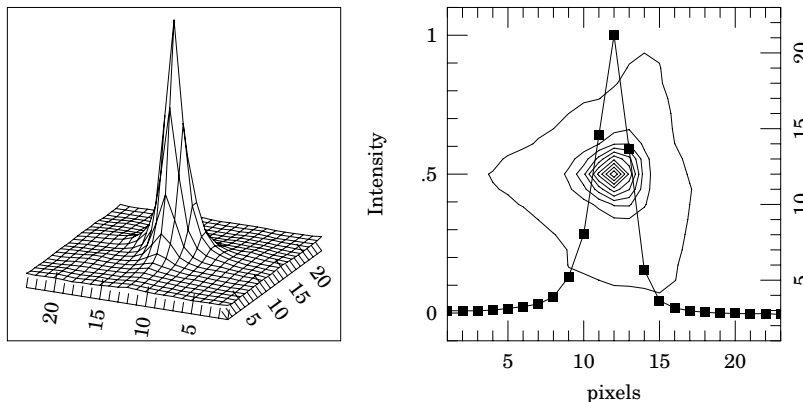


Fig. 1. Point Spread Function of the prototype instrument. Left picture shows mesh plot of the PSF (units are 14.2 arcsec pixels). Right picture shows contour plot of the triangular PSF (isophotes were plotted from intensity 0.01 to 1.01 with 0.1 interval) and its intensity cut (black squares).

Due to the huge pixel size seeing is not a limiting factor for our system. At 14 arcsec per pixel the basic determinant of the PSF size is the lens and mount tracking accuracy. After adjusting the tracking speed of the RA drive we were able to keep the star image centroid within one pixel for at least 20 minutes, much longer than expected exposure time of 3 minutes.

The PSF size and shape were therefore completely determined by the lens quality, which turned out to be of moderate quality. The best focus PSF (Fig. 1) consisted of the sharp, asymmetric (triangular) peak overlayed on the extended wings containing pronounced "fingers". Although its average FWHM is only 2.5 pixels, bright stars' wings are easily traceable to more than 15 pixels from the centroid. Defocusing the lens did not help since it influenced mainly extended feature size.

## 7 Photometry Tests at the Las Campanas Observatory

In March 1997, after obtaining a kind approval from the Carnegie Institution of Washington, we have moved our instrument to the Las Campanas Observatory, Chile, which is operated by the Carnegie Institution of Washington. It was placed in the vicinity of the new telescope (Udalski, Kubiak and Szymański 1997) and room for the control computer was kindly allocated in its control building.

The first testing run started on April 4, 1997 and lasted till April 26, 1997. During the first nights we were able to setup hardware and software, adjust the instrument, take calibration frames and prepare routine observations.



For the test run over twenty  $2 \times 3$  deg fields were selected. They included standard calibration fields (*e.g.*, PG1323-086), crowded fields (in Milky Way and LMC), galaxy rich area (Virgo), ecliptic fields and star-poor regions (Octans).

### 7.1 Aperture vs. Profile Photometry Tests

Two fields were used for photometry tests: crowded field in Centaurus ( $\alpha_{2000} = 11^{\text{h}}35^{\text{m}}00^{\text{s}}$ ,  $\delta_{2000} = -60^{\circ}00'00''$ ) and quite empty field close to the standard field PG1323-086 ( $\alpha_{2000} = 13^{\text{h}}25^{\text{m}}00^{\text{s}}$ ,  $\delta_{2000} = -08^{\circ}50'00''$ ). Over 5000 stars were detected in the Centaurus field and only 600 in the PG1323-086 field.

We have tried both aperture photometry (using our own, combined program for detection, classification and photometry of objects) and profile photometry (DAOPHOT, Stetson 1987) programs. We have also tried DoPhot (Schechter, Mateo and Saha 1993) but without much success because of our non-symmetric PSF.

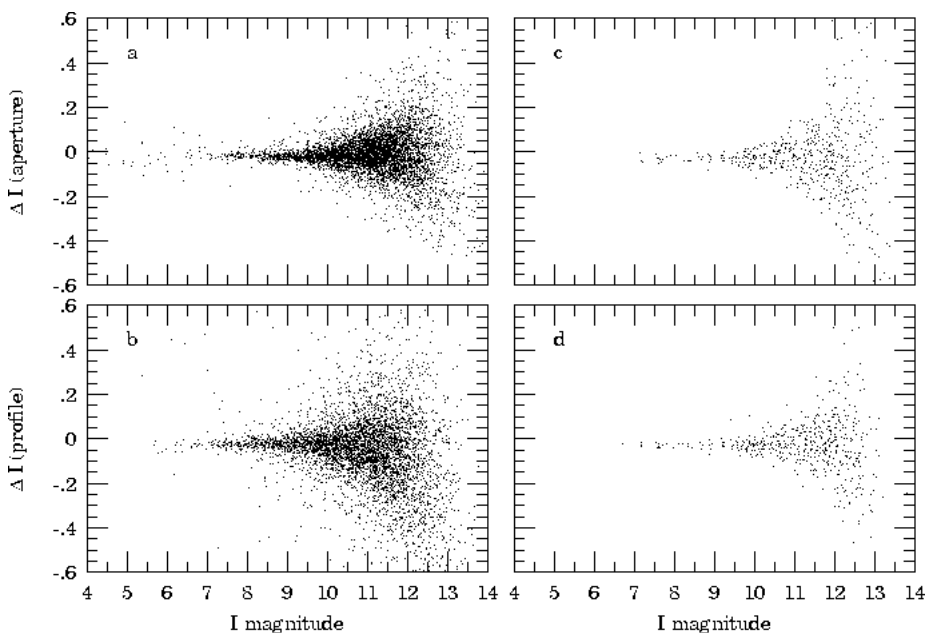


Fig. 2. Magnitude difference measured for the same stars found on two images of the same field: a) and b) aperture and profile photometry of crowded Centaurus field, c) and d) aperture and profile photometry of non-crowded PG1323-086 field.

Fig. 2 presents magnitude difference vs. instrumental  $I$  magnitude for the same stars measured on two images. Left diagrams (a,b) were obtained for the crowded Centaurus field, while right ones (c,d) for PG1323-086 frames. Upper figures (a,c) were obtained using aperture and the lower ones (b,d) using profile photometry.

It is clear from Figs. 2a and 2b, that for crowded fields aperture photometry works much better, at least as far as measurement repeatability is concerned. In empty fields this tendency is reversed – profile photometry gives slightly smaller

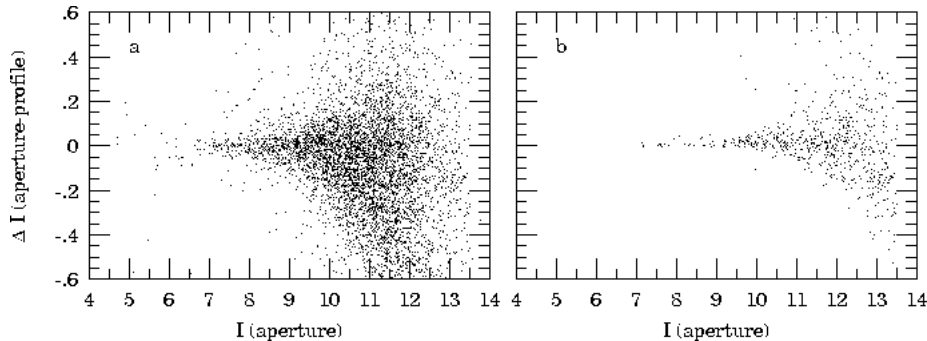


Fig. 3. Difference between profile and aperture photometry for the same frame: a) Centaurus field, b) PG1323-086 field.

magnitude dispersion.

Fig. 3 shows difference between aperture and profile photometry for the crowded (a) and empty (b) fields. In the non-crowded field the dispersion of differences is of the same order as dispersion of measurements obtained using either of methods. There is also a clear linear correspondence between both results. The crowded field data exhibit much larger dispersion and show that for fainter stars linear correspondence between both methods breaks. Both effects are caused partly by aperture photometry errors in crowded field and partly by profile photometry problems in the case of bad PSF.

Since, at least at the present stage of our project, we are much more interested in the variability detection than in the absolute photometry, we decided to use more repeatable aperture photometry. This gives us also strong computational advantage since the aperture photometry in the crowded fields is by factor of 15 faster than profile fitting method.

Stars brighter than 7.5 mag usually contain saturated pixels. However, thanks to the special treatment by our aperture photometry program, we are able to measure also saturated stars, up to about  $I \sim 3$  mag. Obviously rms error of such observations rises significantly and they cannot be brought onto the standard system using general transformation. Nevertheless, differential photometry with  $\sim 0.08$  mag error is feasible.

In Fig. 4 number of stars detected in 0.5 mag  $I$ -band bins in Centaurus field and in all program fields are plotted. Only stars with more than 20 measurements were counted. Data are also listed in Table 1. It is clear, that our present survey is complete to about  $I \sim 11$  mag, and includes more than 30% of 12 mag stars.

## 8 Photometry Results

Fig. 5 shows a plot of the standard deviation in  $I$ -band vs.  $I$  magnitude obtained for over 6000 stars with at least 50 measurements in 160 frames of the Centaurus

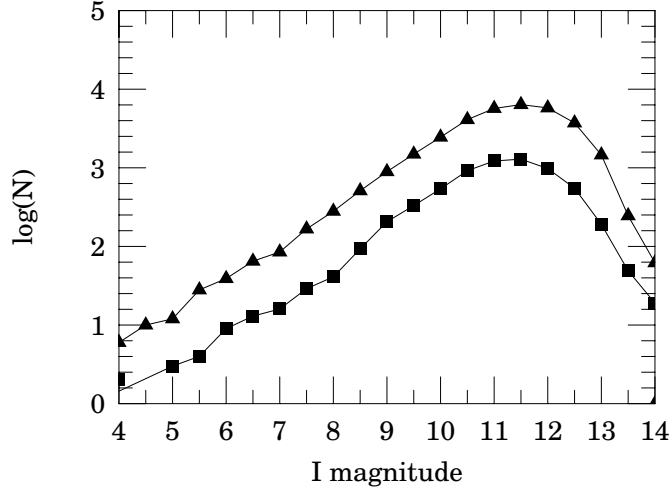


Fig. 4. Number of stars detected in 0.5 mag  $I$ -band bins in Centaurus field (squares) and on all program fields (triangles).

Table 1

Standard deviation envelope of  $I$ -band measurements and number of stars detected in 0.5 mag bins in Centaurus field and in all program fields.

$I$	$\sigma_I$	$N_{\text{Cen}}$	$N_{\text{all}}$	$I$	$\sigma_I$	$N_{\text{Cen}}$	$N_{\text{all}}$
5.0	0.07	3	12	9.5	0.009	331	1495
5.5	0.07	4	28	10.0	0.015	540	2494
6.0	0.07	9	39	10.5	0.019	919	4109
6.5	0.07	13	65	11.0	0.032	1222	5696
7.0	0.06	16	85	11.5	0.045	1288	6378
7.5	0.008	29	167	12.0	0.069	979	5785
8.0	0.008	41	280	12.5	0.105	550	3728
8.5	0.008	93	511	13.0	0.176	191	1459
9.0	0.008	206	895	13.5	0.315	49	246

field. Dispersion increase for stars brighter than about 7 mag caused by saturation, and fast rise for stars fainter than 13 mag are clearly visible. Numbers corresponding to the lower envelope of the data points are listed in Table 1.

In a search for periodic variable stars we restrict ourselves to the stars, that have standard deviation 2 or 3 times larger than the envelope. The number of stars that deviate more than that is still large in Fig. 5. This may indicate some problems with long-term photometric stability.

In Fig. 6 light curves of 8 stars with brightness  $I \sim 6, 7$  (saturated), 8, 9, 10, 11, 12 and 13 mag are plotted. Only stars with small standard deviations (close to

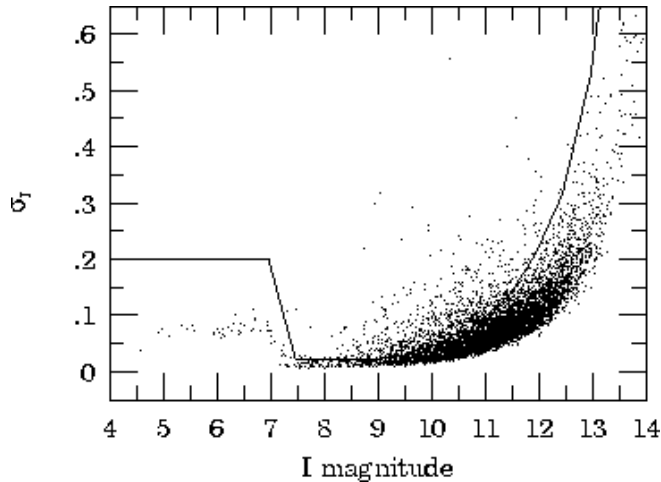


Fig. 5. Standard deviation of  $I$ -band magnitudes vs.  $I$  magnitude in the Centaurus field. Continuous line delimiters stars which standard deviation is larger than three times the envelope value.

the envelope of data points in Fig. 5) were selected, and indeed, they look pretty constant.

Unfortunately this is not the case for all the stars. We have found some cases of the small correlated variations of stellar brightness. An example of such situation is presented in Fig. 7. It shows 6 light curves of a set of 15 stars laying within 15 arc min, for which magnitudes were obtained differentially, so that the mean magnitude of the set remains constant. One can see, that some correlated (and, of course, anticorrelated) variations with amplitude about 0.02 mag occur with the time scales of a few days.

We have looked for possible explanations of this instability but did not find definite answers. The most likely reason is that the sky flat images do not provide proper sensitivity calibration in case of many internal reflections in the lens and improper baffling. We will address this problem during the next run.

Very crude search through our catalog revealed over 70 variables with periods shorter than  $\sim 10$  days; about 50 of them are missing in the General Catalog of Variable Stars (Kholopov *et al.* 1985). Fig. 8 shows four examples of the periodic variables detected above 3 standard deviation threshold using automatic phase dispersion minimization (Stellingwerf 1978) program. Two cycles with zero phase chosen arbitrary are shown. The bottom curve is a seventh magnitude cepheid AY Cen ( $\alpha = 11^{\text{h}}25^{\text{m}}06^{\text{s}}$ ,  $\delta = -60^{\circ}44'04''$ ,  $P = 5^{\text{d}}.30975$ ). Three other are newly discovered quite bright variables: W UMa type ( $\alpha = 11^{\text{h}}29^{\text{m}}43^{\text{s}}$ ,  $\delta = -63^{\circ}23'09''$ ,  $P = 0^{\text{d}}.9444$ ), Algol type ( $\alpha = 11^{\text{h}}26^{\text{m}}12^{\text{s}}$ ,  $\delta = -62^{\circ}10'14''$ ,  $P = 1^{\text{d}}.3164$ ) and SAO 204959 ( $\alpha = 13^{\text{h}}53^{\text{m}}40^{\text{s}}$ ,  $\delta = -30^{\circ}36'02''$ ,  $P = 0^{\text{d}}.4761$ ), other W UMa type star.

Detailed catalog of the variable stars detected during the Las Campanas test will be published elsewhere. At present it is available over the Internet:

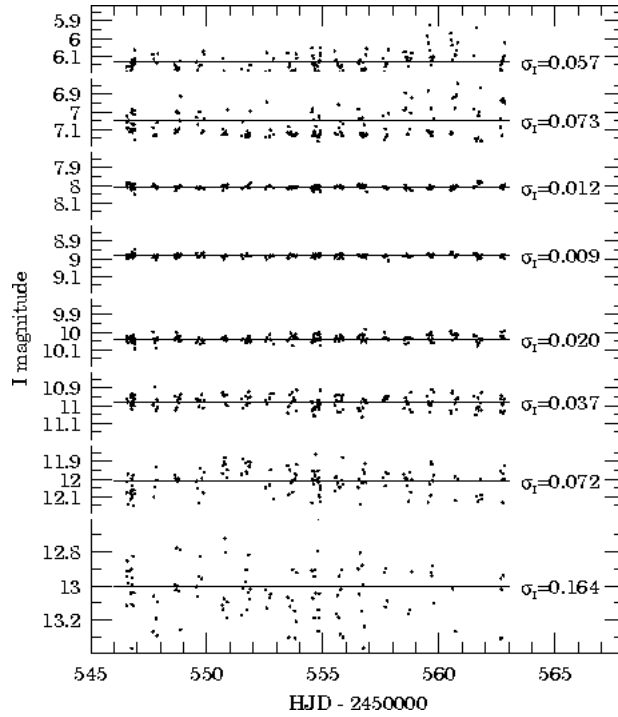


Fig. 6. Light curves for 8 non-variable stars in the magnitude range  $I \sim 6 \text{ mag} - 13 \text{ mag}$ . Abscissa values cover 0.4 mag ranges for each star (0.8 mag for 13 mag star). Two brightest stars are saturated. Stars were selected to have standard deviations ( $\sigma_I$ ) close to the envelope from the Fig. 5.

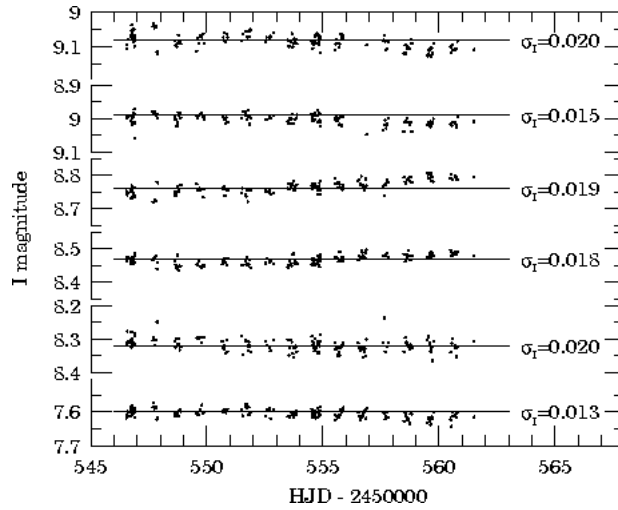


Fig. 7. Light curves of 6 out of 15 non-variable stars laying with 15 arc min. Raw stellar magnitudes were transformed to the common system in which average magnitude of the set does not change. Some long-term, correlated variations are present.

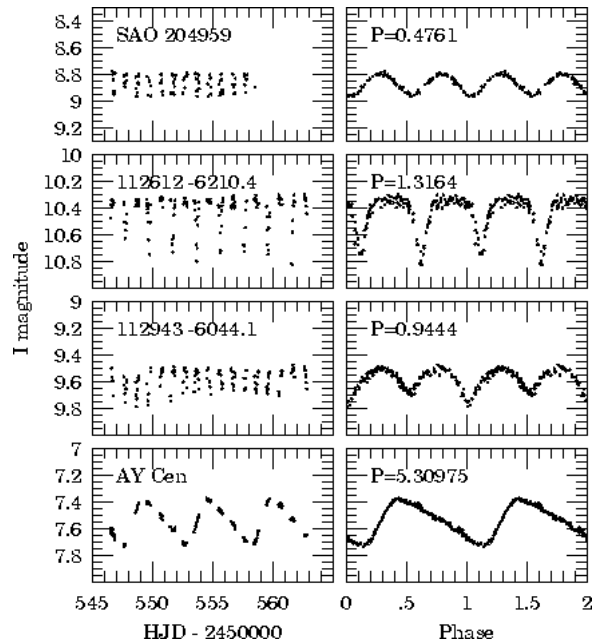


Fig. 8. Four examples of the periodic variables detected during the Las Campanas test run. Left diagrams show  $I$ -band magnitude vs. heliocentric Julian Data (HJD), while the right ones – phased light curves. Periods were determined using PDM technique. Only AY Cen was previously known to be variable.

<http://www.astrouw.edu.pl/~gp/asas/variables.html>.

## 9 Conclusions and Prospects

Using a very simple and inexpensive equipment we were able to monitor large area of the sky in the fully automatic way.

During our test run at the Las Campanas Observatory we have monitored over 150 sq. degrees of the sky. Each night 5 to 10 exposures of each field were obtained, resulting in over 30 000 stars observed more than 50 times each. In present configuration (14 arcsec/pixels) our observations were sky limited, but nevertheless 12 mag limit was easily achieved using 135/1.8 telephoto lens. Photometry results were acceptable although some unidentified source of small errors excludes at the moment precise data calibration. We estimate, that differential photometry is accurate to about 0.02 mag for the brightest stars, but we cannot bring our current  $I$ -band magnitudes closer than 0.05 to the standard values.

The next step of our project will be to exchange our small ( $512 \times 768$ ) CCD detector for the much larger one ( $2k \times 2k$ ), what will immediately result in 10 times increased data flow. We will upgrade our computing power to be able to reduce data flow of 1 GB per night. This way we will be able to monitor over 6000 sq. degrees per night with only one instrument. Once we get it working we are

going to clone the system and place several copies of it in a few good observing sites. Having a few instruments running we will use different filters, to obtain, not available now, multiwavelength photometry.

We are going to reduce human interaction with the system to the minimum. Next generation instruments will be protected by automatic, self controlled enclosures. Users will interact remotely only with the final photometric database. We also plan to add an early detection system to our database software to detect that exceptional events in the real time.

**Acknowledgements.** It is a great pleasure to thank Prof. Bohdan Paczyński for initiative in this project, providing necessary funds and creative contribution at all stages of the project.

We would like to thank Drs. Augustus Oemler and Miguel Roth from the Observatories of the Carnegie Institution of Washington for letting us use the Las Campanas Observatory facilities and offering invaluable support at the site.

We are indebted to Drs. Marcin Kubiak and Andrzej Udalski for letting us use facilities of the telescope to house our prototype device, to Dr. Michał Szymański for programming advice and computer system set up, and to all members of the OGLE team for continuous care of our instrumentation.

This work was partly supported by the KBN BST grant.

## REFERENCES

- Alcock, C., *et al.* 1993, *Nature*, **365**, 621.  
 Aubourg, E., *et al.* 1993, *Nature*, **365**, 623.  
 Braeuer, H.-J., and Vogt, N. 1995, *Proceedings of IAU Colloquium*, No 151, ed. J. Greiner, H.W. Duerbeck and R.E. Gershberg, 402.  
 Genet, R.M., and Hayes, D.S. 1989, "Robotic Observatories", Mesa, AutoScope Corp.  
 Gunn, J.E., and Knapp, G.R. 1993, in *Astronomical Surveys*, ed. B.T. Soifer, *ASP Conference Proceedings* **43**, 267.  
 Henry, G.W., and Eaton, J.A. eds 1995, "Robotic Telescopes: Current Capabilities, Present Developments and Future Prospects for Automated Astronomy".  
 Kholopov, P.N., *et al.* 1985, General Catalog of Variable Stars, The Fourth Edition, Nauka, Moscow.  
 Schechter, P.L., Mateo, M., Saha, A. 1993, *P.A.S.P.*, **105**, 1342.  
 Paczyński, B. 1997, "The Future of Massive Variability Searches", in *Proceedings of 12th IAP Colloquium: "Variable Stars and the Astrophysical Returns of Microlensing Searches"*, Paris (Ed. R. Ferlet), p. 357.  
 Schaefer, B.E., *et al.* 1994, *Astrophys. J. Letters*, **422**, L71.  
 Stellingwerf, R.F. 1978, *Astrophys. J.*, **224**, 953.  
 Stetson, P.B. 1987, *P.A.S.P.*, **99**, 191.  
 Stetson, P.B., and Lazaro, C. 1990, *Astron. J.*, **99**, 983.  
 Udalski, A., *et al.* 1992, *Acta Astron.*, **42**, 253.  
 Udalski, A. Kubiak, M., and Szymański, M. 1997, *Acta Astron.*, **47**, 319.  
 Van Dyck, S.D., Treffers, R.R., Richmond, M.W., Filippenko, A.V., Paik, Y. 1994, *Bulletin of the American Astronomical Society*, **185**, 79.05.